Astron. Astrophys. 243, 531–545 (1991)

ASTRONOMY AND ASTROPHYSICS

The simulation of Forbush decreases with time-dependent cosmic-ray modulation models of varying complexity

J.A. le Roux and M.S. Potgieter

Department of Physics, Potchefstroom University for CHE, 2520 Potchefstroom, South Africa

Received April 23, accepted October 4, 1990

Abstract We developed an axially-symmetric time-dependent numerical drift model with a simulated wavy neutral sheet with which Forbush decreases (Fd's) were modelled by assuming that they were caused by propagating regions of enhanced scattering and diminished drift. We studied the magnitude and recovery times of Fd's in the intensity of 1 GeV protons in the equatorial plane as a function of radial distance by varying the complexity of the models. The model was first tested against the linear analysis of Chih & Lee (1986) by simplifying it to a one-dimensional (1D) model. This model behaved qualitatively in accordance with the results of the linear analysis. Quantitative differences were the result of the assumptions upon which the linear analysis was based. To simulate a realistic Fd at Earth it was necessary to simulate a propagating disturbance that became less effective in sweeping away inward diffusing particles at larger radial distances. The decrease in the magnitude and the increase in the recovery time of Fd's with increasing radial distance corresponded qualitatively with observations (Webber et al. 1986). The radial dependence of the magnitude was however predicted much too strong contrary to the observations. Application of the two-dimensional (2D) model without drift showed that the magnitude of the Fd adhered qualitively to the local value of a linear combination of parallel and perpendicular diffusion coefficients. The radial dependence of both the magnitude and the recovery time of the Fd showed a promising compatibility with the data. This improvement was a natural consequence of the important role of crossfield diffusion and the 2D geometry of the disturbance. The predicted increase of the recovery time with radial distance was also determined by the developing geometry of the propagating disturbance because, although the disturbance had a fixed radial and latitudinal extent at all radial distances, it acquired an area which increased linearly with increasing radial distance in a spherical coordinate system. The 2D model with drift included was remarkably successful in giving a realistic intensity-time profile of Fd's at Earth considering the additional complexity of drift in the model. The calculated recovery times of Fd's at Earth, however, were noticeably longer during the epoch when the northern-hemisphere interplanetary magnetic field (IMF) pointed towards the Sun ($A < 0$) than during the epoch when the northern-hemispheric IMF pointed away from the Sun ($A > 0$) and for a small neutral sheet tilt angle corresponding to solar minimum conditions. The polarity-reversal effect was found too large compared with observations. We showed for the first time that the polarity-reversal effect was reduced substantially when the tilt angle was increased corresponding to solar maximum conditions. This effect, however, was still too large. Consequently, three modifications to the drift model namely, a solar polar field deviation from the Parker spiral field, decaying disturbances as a function of radial distance and reduced drift (factor of 3) were considered. The best results compared with observations were obtained with reduced drift because not only was the polarity-reversal effect on the recovery time reduced significantly at Earth, but a reasonable correlation of the magnitude and the recovery time of Fd's with observation as a function of radial distance in the equatorial plane was achieved.

Key words: cosmic rays: Forbush decreases– heliospheric modulation– Sun: activity of

1. Introduction

The subject of this paper is the classical Forbush decrease (Fd) in the intensity of galactic cosmic rays observed in the heliosphere and which has the well known asymmetrical pattern of a sudden decrease in a few hours and an almost exponential recovery of a few days.

Since it had been established that Fd's were not due to geomagnetic influences, but rather to solar activity, early theoretical work suggested various mechanisms to explain these phenomena and had established in the process all the important mechanisms of cosmic-ray modulation. Morrison (1956), for example, was the first to suggest that Fd's could be caused by turbulent magnetic clouds ejected from solar active regions. Singer (1958) and Laster et al. (1962) proposed cosmic rays temporarily trapped in an expanding turbulent magnetic cloud being adiabatically cooled. Parker (1963) showed that the ambient interplanetary magnetic field (IMF) would be compressed and distorted by a shock wave, forming a shell of intense magnetic fields which could act as a shield against incoming cosmic rays. In this blast wave model he also considered the additional effects of diffusion and large scale gradient drift. All these and other mechanisms were later combined by Parker (1965) in the well known fundamental transport equation (TPQ) of cosmic rays in the heliosphere. Since then the emphasis has been on the understanding of the 11-year solar modulation through the steady state solutions of this equation. Since the 1970's the continual satellite coverage of the solar wind properties and cosmic ray intensities at various positions in or

Send offprint requests to: M.S. Potgieter

near the equatorial plane has, however, led to a renewed interest in finding the dominating mechanism of Fd's amongst the existing ones. This is especially due to the revival of the original idea of Lockwood (1960) that the 11-year modulation cycle could be the result of the accumulation of many Fd's caused by propagating interplanetary disturbances. Up to now no consensus has been reached on the main mechanism that causes Fd's. Although the idea of Fd's caused by enhanced scattering in disordered magnetic fields in the vicinity of shocks [actually a revival of the Morrison (1956) argument] has been more popular in recent models (e.g., Nishida 1983; Lockwood et al. 1986; Chih & Lee 1986), the experimental evidence is not conclusive. On the one hand, there are those who favour enhanced scattering (e.g., Zhang & Burlaga 1986; Badruddin & Yadav 1986), while others (e.g., Sarris et al. 1988) argue for drift caused by gradients in the relative large-scale ordered magnetic fields of propagating solar wind disturbances as the driving mechanism of Fd's.

Apart from the uncertainties about what the main mechanism of Fd's is, the presence of spacecraft at large radial distances in the heliosphere raised the question whether Fd's could be detected at these distances and, if so, what the radial dependence of the magnitude (maximum %-decrease) and the recovery time of Fd's would be. This also is a complex problem considering the few satellites present in the heliosphere and the difficulty of a correct interpretation of the available experimental data. However, Van Allen (1979) was the first to notice that the recovery time of a Fd seemed to be much longer at larger radial distances (~ 16 AU) in the heliosphere than at Earth. Two different viewpoints have since been advanced as a possible explanation for this observation. On the one hand, Burlaga et al. (1985) claim that it is a matter of many Fd's following each other in close succession, and which, when forming so-called merged interactive regions (MIR's), may cause long recovery times at larger radial distances rather than a single Fd which recovers slowly behind a heliospheric shock. In other words, the disturbance which originally caused a Fd at Earth has evolved and coalesced with other disturbances at larger distances in such a way as to form a new dynamical system in which the original disturbance loses its identity. According to them, it may therefore not be possible to follow an isolated disturbance outwards to large radial distances and to comment on the recovery time and the magnitude of the decrease it causes in the intensity of galactic cosmic rays.

Lockwood & Webber (1987), on the other hand, claim that they traced a large isolated transient disturbance radially outwards from 1 AU to ~ 35 AU during 1986. Since there were no other significant disturbances which passed Earth 6 months prior to the one studied they argued that merging effects could not have been of any importance. They gave for $E > 60$ MeV protons a detailed radial dependence for the magnitude of the isolated Fd and its recovery time near the equatorial plane showing that the recovery time which averaged ~ 5 d at 1 AU was 20 times longer at 30 AU, while the magnitude of the decrease at 30 AU was only a factor 2 smaller than at Earth. These results compare favourably with those of Webber et al. (1986) for 20 large Fd's with magnitude $> 10\%$ observed between 1–30 AU from 1978–1984 when the Sun was more active and merging effects probably more important. It may be, as was suggested by them, that the longer recovery times of Fd's at larger radial distances are a geometrical effect related to the larger volume in space occupied by the preceding disturbance at these radial distances and that merging effects play only a secondary role. From these opposing arguments it is evident that discrepancies, and even controversies, exist about the causes *and the detection* of Fd's and that further investigations are essential. The stimulation from interplanetary observations has led more recently to a greater emphasis on time-dependent numerical solutions of the TPQ and to the consequent development of sophisticated time-dependent numerical models which could be used to study the Fd both as an isolated event (which will be studied in this paper) as well as the effect of the accumulation of Fd's on the long-term modulation of cosmic rays (which will be addressed elsewhere).

Next, a brief review is given of some important papers which appeared on the subject of the simulation of an isolated Fd. Nishida (1982), for example, solved the one-dimensional (1D), time-dependent, diffusion-convection equation numerically in spherical coordinates neglecting adiabatic cooling. In his model the Fd was caused by a region of enhanced scattering and convection behind an interplanetary propagating shock wave. The enhanced scattering (decreased diffusion path length) was found more effective than the enhanced convection in causing the Fd. The magnitude of the Fd was found to be determined by the value of the diffusion coefficient just in front of the propagating disturbance. An increase in the positive radial dependence of the diffusion coefficient resulted in an increase in the rate at which the magnitude of the Fd decreased with the outward propagating disturbed region, and a consequent increase in the recovery rate of the Fd at 1 AU. Recently, Perko (1987), using a complete 1D time-dependent model but with a radially independent diffusion coefficient, briefly discussed the recovery rate of a Fd at Earth. He pointed out that a weakening of the propagating disturbance was not necessary for an immediate recovery to follow the decreased intensity as for a typical Fd at Earth. This was contrary to the findings of both Chih & Lee (1986) and Lockwood et al. (1986) who used a weakening disturbance in their models to simulate a realistic Fd at Earth. In a totally different approach Thomas & Gall (1984) used Monte Carlo techniques to study Fd's. In their model the solar-flare induced travelling shock wave disturbance was represented by a region of enhanced magnetic field strength with a longitudinal as well as a radial extent. This allowed them to make statements about the dependence of the magnitude and the recovery time of a Fd upon the diffusion mean free path as well the geometry of the shock wave at 1 AU for relativistic cosmic-ray protons. They found that the magnitude of the Fd diminished with an increase in the diffusion mean free path as well as a decrease in the longitudinal dimension of the shock wave. The recovery time of the simulated Fd was not strongly dependent on the mean free path, but depended largely on the geometry of the shock wave, because the recovery time became significantly longer when the longitudinal dimension of the disturbance was increased. They also concluded that the prolonged containment of cosmic-ray particles in the region between the flare shock wave and the Sun, leading to additional adiabatic cooling, is the principal mechanism in causing Fd's.

With the rapid improvement of computer power the employment of relative advanced numerical methods became a reality. Kadokura & Nishida (1986) solved the two dimensional (2D), time-dependent TPQ, with drift included, numerically using a flat heliospheric neutral sheet. Their model of radially propagating interplanetary disturbances were associated with enhanced convection, enhanced scattering (enhanced variability in the IMF behind the shock front) as well as the enhancement of the magnitude of the IMF (the result of a kink in the field at the shock front). The dominating mechanism causing the Fd was found to be the increase in the IMF during the passage of the disturbance. The inclusion of drift allowed them to make predictions about the effect of the IMF's polarity change on the magnitude and the recovery time of Fd's, but only near Earth. According to their model the magnitude of the Fd was smaller and the recovery time clearly longer when the northern-hemispheric IMF points towards the Sun ($A < 0$) than when the northern-hemispheric IMF points away from the Sun ($A > 0$). The latter is in disagreement with observations where no (Lockwood et al. 1986) or only a barely statistically significant effect (Mulder & Moraal, 1986) on the recovery time was detected after the polarity of the IMF reversed. Lockwood et al. (1986), also using a 2D time-dependent numerical model with drift and a flat neutral sheet, commented briefly on the effect of the polarity change of the IMF on the recovery of a Fd at 1 AU and reported only a minor change in the recovery time when the polarity of the IMF was reversed in apparent agreement with observations. In their model, however, the propagating disturbance decayed as $e^{-r/7}$, with r in AU, so that the reason for this minor change was that the recovery of the Fd depended primarily on the decay of the disturbance and only secondary on the transport parameters of the disturbance. The implication of such a strong decay of the disturbance with radial distance is that the magnitude of Fd's will have a strong radial dependence contrary to the weak radial dependence observed by Webber et al. (1986). This aspect will be discussed in more detail later.

On the analytical side, Chih & Lee (1986) solved the time-dependent, diffusion-convection equation under the assumption of small temporal variations in the modulation parameters and the cosmic ray intensity, and neglecting particle energy changes as well as drift transport. They considered the temporal variation of only the diffusion coefficient when the interplanetary disturbance passed the observer. Despite the relative simplicity of the model their work on the magnitude and recovery of Fd's has been extremely valuable in providing a first order test for the more complex numerical models and giving insights not so easily obtained with numerical work.

From this review it is evident that no definite conclusion can be drawn about the dominant mechanism in interplanetary disturbances which cause Fd's. No attempt has yet been made to simulate Fd's numerically at larger distances in the equatorial plane, partly because of scant experimental data and partly because numerical studies with time-dependent models are extremely time-consuming on a computer at present. Also, the characteristics of the Fd as a function of the neutral sheet waviness has not been addressed in model studies (or data analyses) before. In an attempt to address some of these issues, especially the latter, we developed our own 2D time-dependent modulation model based on the numerical solution of the TPQ with the effects of a simulated wavy neutral sheet incorporated. (Preliminary results were reported by Le Roux & Potgieter 1989, 1990a.) The details of this model will be presented in Sect. 2. In Sect. 3 we shall discuss the simulation of the Fd in the simplified 1D (spherically-symmetric) version of the model and use the opportunity to compare our results with the analytical model of Chih & Lee (1986) to establish the reliability and consistency of our model. In Sect. 4 the results of the 2D non-drift model concerning the magnitude and the recovery time of the Fd, especially as a function of radial distance, are presented and compared with the results of the 1D model. Comparison of the predictions of both the 1D and 2D non-drift models with observations are also made. In Sect. 5 the effects of drift and a wavy neutral sheet on the magnitude and the recovery times of Fd's are compared with those of the 2D non-drift model. Calculations illustrating the dependence on the polarity-reversal of the IMF and the neutral sheet tilt angle, α, are presented for the first time. Special attention will be given to the effect of the polarity change of the IMF on the recovery time of a simulated Fd at Earth and to comparison with observations. A summary and conclusions are given in Sect. 6.

2. The general model

The TPQ for the modulation of cosmic rays in the heliosphere (Parker 1965) is now widely accepted and used. This equation, in a heliocentric spherical coordinate system (r, θ, ϕ), assuming azimuthal symmetry is:

$$\begin{aligned}\frac{\partial f}{\partial t} &= K_{rr}\frac{\partial^2 f}{\partial r^2} + \frac{1}{r^2}K_{\theta\theta}\frac{\partial^2 f}{\partial \theta^2} \\ &+ \left[\frac{1}{r^2}\frac{\partial}{\partial r}(r^2 K_{rr}) + \frac{1}{r\sin\theta}\frac{\partial}{\partial\theta}(\sin\theta K_{\theta r}) - V\right]\frac{\partial f}{\partial r} \\ &+ \left[\frac{1}{r^2}\frac{\partial}{\partial r}(rK_{r\theta}) \right.\\ &\left. + \frac{1}{r^2\sin\theta}\frac{\partial}{\partial\theta}(\sin\theta K_{\theta\theta})\right]\frac{\partial f}{\partial\theta} \\ &+ \frac{1}{3r^2}\frac{\partial}{\partial r}(r^2 V)\frac{\partial f}{\partial \ln P}. \end{aligned} \tag{1}$$

We solved this equation for the omnidirectional distribution function $f(r, \theta, P, t)$ with respect to radial distance r, polar angle θ, rigidity P and time t, where the differential intensity is $j_T \propto P^2 f$; V represents the radially directed solar wind velocity. To allow for the generally accepted increase in V with latitude we used the form $V = 400(1 + \cos^2\theta)$ km s^{-1} when $45° \le \theta \le 90°$, and $V = 600$ km s^{-1} when $0° \le \theta < 45°$ (Zhao & Hundhausen 1983). The coefficients $K_{rr} = K_{\parallel}\cos^2\psi + K_{\perp}\sin^2\psi$ and $K_{\theta\theta} = K_{\perp}$ are the diagonal elements of the diffusion tensor where $K_{\parallel}$ and $K_{\perp}$ respectively represent the diffusion coefficients parallel and perpendicular to the mean IMF and ψ the angle between the radial and mean IMF directions. The coefficients $K_{r\theta}$ and $K_{\theta r}$ are the off-diagonal elements of the diffusion tensor and can be expressed as $K_{r\theta} = -K_{\theta r} = -K_T \sin\psi$, where K_T describes the effects of particle gradient and curvature drift in the large-scale IMF. We accepted the standard Archimedian (or Parker) spiral pattern for the IMF given by

$$\boldsymbol{B} = \frac{B_0}{r^2}[\boldsymbol{e}_r - \tan\psi \boldsymbol{e}_\phi].$$

Here, $\boldsymbol{B}_0$ is the magnetic field strength at Earth (taken as 5 nT) and, $\tan\psi = \Omega(r - r_0)\sin\theta/V$, with Ω the angular velocity of the Sun about its rotation axis and $r_0 = 0.1$ AU. For the diffusion coefficients parallel and perpendicular to the background IMF we assumed respectively

$$K_{\parallel} = K_0 \beta K_p(P) B_0/(3B), \tag{2a}$$

and

$$K_{\perp} = 0.05 K_{\parallel}, \tag{2b}$$

with $K_p(P) = P$, if $P > P_0$; $K_p(P) = P_0$, if $P \leq P_0$, and K_0 a constant, which will be specified later, in units of $6\,10^{20}\,\mathrm{cm^2\,s^{-1}}$; $\beta = v/c$, with v the particle velocity and c the velocity of light; $P_0 = 0.4\,\mathrm{GV}$ and $B = |\boldsymbol{B}|$. For the drift coefficient we used

$$K_T = (K_T)_0 \beta P/(3B)\,, \tag{3}$$

with $(K_T)_0$ a dimensionless constant equal to one for full drift and less than one for reduced drift effects. These choices for the elements of the diffusion tensor are simple to handle and seem reasonable considering the little known about their spatial and rigidity dependence.

In our model the outer boundary of the heliosphere is situated at 50 AU where a local interstellar proton spectrum was assumed as

$$j_T = 6.7\left[\frac{T^{0.7}}{(T+0.25)^3}\right], \tag{4}$$

with T the kinetic energy of the cosmic-ray protons. At 0.1 AU we assumed the inner boundary condition as $\partial f/\partial r = 0$, and at the heliospheric pole ($\theta = 0°$) we assumed symmetry of the IMF so that $\partial f/\partial \theta = 0$.

In modelling the neutral sheet in the equatorial plane, it was decided to use the method of Potgieter (1984) – see also Potgieter & Moraal (1985). Although a warped neutral sheet is not physically present in this model it simulates the effects of such a sheet on the intensity of cosmic rays and gives the same general effects as a three dimensional model with a warped neutral sheet (for details, see Burger & Potgieter, 1989). This leads to a large reduction in the computer time needed to complete a simulation. The usefulness of the method was also greatly extended when the results generated with the method was quantified in terms of the tilt angle, α, of the wavy neutral sheet by Burger & Potgieter (1989) – the tilt angle is defined as the excursion of the wavy neutral sheet from the rotational equator of the Sun at a particular time. This enabled us to study the characteristics of the Fd at different levels of neutral sheet waviness leading to new results as will be illustrated in the next section. The method is limited only in the sense that it averages over 27 days and can therefore not simulate periodicities of 27 days and shorter.

Equation (1) was solved numerically with the alternating direction implicit (ADI) method (Fisk 1976), but extended to include time-dependence. The steady-state solution of the TPQ served as the initial condition for the time-dependent numerical code. The number of grid points employed in (r, θ, P) were $(800, 19, 22)$ respectively. We used a non-linear grid in polar angle θ (from $\theta = 0°-90°$) with the smallest distance between grid points close to the neutral sheet since we were mainly concerned with studying Fd's in the equatorial regions. A non-linear grid was also employed with respect to rigidity P with the largest steps at the higher rigidities where little modulation was assumed. Calculations were performed, from 10 GV (9.1 GeV) down to 1.7 GV (1 GeV), using very small time-steps, $\Delta t = 6.5\,\mathrm{h}$, in order to ensure a good time-resolution for the calculated intensities of the Fd.

In view of the success of the enhanced scattering approach (incorporated as a decrease in the mean free path or diffusion coefficient) for simulating Fd's in both ID and 2D time-dependent models (e.g., Nishida 1982; Chih & Lee 1986) it was decided, for this paper, to analyse the effect of this mechanism in more detail with our model. We therefore assumed a radially propagating disturbance in which the diffusion coefficients $K_\parallel$, $K_\perp$ and the drift coefficient K_T [Eqs. (2a), (2b) and (3)] were decreased simultaneously. The drift coefficient was decreased in the disturbed region because drift should become less effective with enhanced scattering. Since most transient solar activity is thought to be near and around the equatorial plane our disturbance was released from the Sun's equator at $\theta = 90°$ to travel radially outwards along the equatorial plane at $400\,\mathrm{km\,s^{-1}}$ reaching the modulation boundary at 50 AU after about 215 days. The disturbance was given a radial extent L (in AU) and an amplitude $D(\theta)$ which also determined the latitudinal extent of the disturbance above and below the equatorial plane. Inside the outward propagating disturbed region the elements of the diffusion tensor were assumed to vary sinusoidially as

$$K'_{\parallel,\perp,T} = K_{\parallel,\perp,T}\left[1 - D(\theta)\sin^2\left(\frac{\pi r_\mathrm{d}}{L}\right)\right], \tag{5}$$

with $0 \leq r_\mathrm{d} \leq L$. Here, r_d is the radial distance in the disturbance, and $D(\theta) = D_\mathrm{m}[1 - \mathrm{e}^{k(\theta-\theta_\mathrm{m})}]$ for $\theta_\mathrm{m} \leq \theta \leq 90°$ and $D(\theta) = 0$ for $\theta < \theta_\mathrm{m}$; D_m is the maximum amplitude of the disturbance, θ_m is the polar angle at which the disturbance commences and k is a constant. The expression for $D(\theta)$ therefore ensured that D_m was assigned to the equatorial plane and that $D(\theta)$ decreased gradually with decreasing polar angle until it became zero at $\theta = \theta_\mathrm{m}$; D_m was set at 0.9 implying a maximum decrease of a factor of 10 in the diffusion and drift coefficients in the equatorial plane during the passage of the disturbance. We employed a disturbance with $L = 1\,\mathrm{AU}$ and a latitudinal extent of 15° above and below the equatorial plane, i.e., $\theta_\mathrm{m} = 75°$. Although the dimensions of such a travelling disturbance are unknown we consider this a reasonable choice (see also Burlaga et al. 1985).

3. The simulation of Fd's with a spherically-symmetric model

Spherical symmetry is automatically achieved in our model when drift (K_T) and crossfield diffusion ($K_\perp$) are neglected. This gives the opportunity to compare our results on the magnitude of an isolated radially propagating Fd and its recovery time as a function of radial distance with the 1D analytical results of Chih & Lee (1986). Their results provide a valuable test to evaluate our model as well as a fundamental understanding of which parameters determine the magnitude and recovery time of a Fd. They assumed that a Fd was caused by the passage of a region in which the diffusion coefficient was depressed due to an interplanetary travelling shock. From their work it first follows that in the present version of our numerical 1D model the magnitude of the Fd at a particular position in the heliosphere should be determined in general by

$$\left(\frac{\Delta j_T}{j_T}\right)_{\max} = \frac{V\left(\dfrac{\Delta K_{rr}}{K_{rr}}\right)L}{K_{rr}}, \tag{6}$$

where ΔK_{rr} is the depression in K_{rr} in the disturbed region so that $(\Delta K_{rr}/K_{rr})$ is the magnitude of the disturbance. The local value of K_{rr}, i.e., the value at an observation point, plays therefore a crucial role in determining the magnitude of the Fd which a disturbance can cause. If K_{rr} increases with radial distance, and with the other parameters fixed, $(\Delta j_T/j_T)_{\max}$ will decrease accordingly; with K_{rr} independent of radial distance the magnitude of the Fd will be the same throughout the heliosphere. Second, when $r < V_\mathrm{s}t$, with t the total travelling time and V_s the propagating speed of the disturbances, Eq. (6) describes the intensity recovery phase of the Fd as seen by the observer from the moment the disturbed region passes by. The practical application of this is that the recovery time of a Fd can be calculated by using Eq. (6).

As a first example, let the magnitude of the disturbance decrease exponentially with increasing radial distance like $e^{-r/S}$, with S the scale length of the decay. With the rest of the parameters independent of r, Eq. (6) becomes

$$\left(\frac{\Delta j_T}{j_T}\right)_{\max} = k e^{-r/S}, \quad \text{with } k = \frac{VL}{K_{rr}} = \text{constant}.$$

For this situation, $(\Delta j_T/j_T)_{\max}$, the magnitude of the Fd, will also decrease exponentially with increasing radial distance. To address the recovery time, t_r, of the Fd which is defined as the time it will take the Fd to recovery to $\frac{1}{3}$ of its maximum decrease, one can argue as follows: the recovery time at r_1 is equal to the time the disturbance has travelled to produce a Fd, at r_2, which has a magnitude of $\frac{1}{3}$ of its magnitude at r_1, i.e., when $(\Delta j_T/j_T)_{\max}(r_2) = \frac{1}{3}(\Delta j_T/j_T)_{\max}(r_1)$. Therefore,

$$\frac{\left(\frac{\Delta j_T}{j_T}\right)_{\max}(r_2)}{\left(\frac{\Delta j_T}{j_T}\right)_{\max}(r_1)} = e^{-(r_2-r_1)/S} = \frac{1}{3} \simeq e^{-1}, \tag{7}$$

implying that under this condition, $S \simeq (r_2 - r_1)$, so that the recovery time is

$$t_r = \frac{r_2 - r_1}{V_s} \simeq \frac{S}{V_s}. \tag{8}$$

This result shows that a disturbance propagating with a fixed speed and fixed scale length of decay will cause a Fd with a recovery time independent of radial distance. As a second example, let $K_{rr} = k_1 r$, with k_1 a constant and the rest of the modulation parameters in (6) independent of r. This gives

$$\left(\frac{\Delta j_T}{j_T}\right)_{\max} = \frac{k}{r}, \quad \text{with } k = \frac{V\left(\frac{\Delta K_{rr}}{K_{rr}}\right)L}{k_1} = \text{constant}.$$

Then,

$$\frac{\left(\frac{\Delta j_T}{j_T}\right)_{\max}(r_2)}{\left(\frac{\Delta j_T}{j_T}\right)_{\max}(r_1)} = \frac{r_1}{r_2} = \frac{1}{3}, \tag{9}$$

so that $r_2 = 3r_1$ and the recovery time is

$$t_r = \frac{2r_1}{V_s}. \tag{10}$$

This means that the recovery time increases linearly with radial distance although the disturbance's amplitude and radial extent do not change with r. It illustrates that the effectiveness of the disturbance in forming a barrier against the enhanced diffusion of radially inward diffusing particles decreases at larger radial distances. Thirdly, if all the parameters in Eq. (6) are kept unchanged with radial distance, $(\Delta j_T/j_T)_{\max}$ = constant, and the prediction is that no recovery whatsoever will take place anywhere behind the disturbance. These three examples illustrate two interesting fundamental aspects of short-term modulation effects like Fd's in 1D time-dependent models: (1) That the magnitude of the decrease is determined by the local modulation conditions (e.g., V, K_{rr}) and characteristics of the disturbance (e.g., L and $\Delta K_{rr}/K_{rr}$). (2) The recovery, on the other hand, being less abrupt than the decrease is determined not by local parameters, but by the modulation conditions which the propagating disturbance encounters between the observer and the modulation boundary, and by the evolution of the disturbance's characteristics during the propagating process.

These three examples provide a general test for the correctness of our model. It is, however, not expected that there should be anything more than a qualitative agreement between the predictions of the analytical 1D model of Chih & Lee (1986) and our numerical 1D model taking into account that in their model energy changes of cosmic rays were neglected, while in the numerical model adiabatic cooling was included. The results of this comparison will be shown in Fig. 1 to 4. In these and all the other figures in this paper the magnitude of the Fd were calculated by considering the undisturbed (or pre-Fd) intensity level, j_0, i.e., before the passage of the disturbance and the minimum intensity level, j_1, caused by the propagating disturbance, so that $(\Delta j_T/j_T)_{\max} = (j_0 - j_1)/j_0$, and the recovery time as defined earlier. For all the figures in this section a value of 7.7 was used for K_0 in Eq. (2a).

In Fig. 1a and b respectively the magnitude and the recovery time of the Fd as a function of radial distance in the equatorial plane are shown as calculated for 1 GeV protons. As in the first example we let the magnitude of the disturbance, $(\Delta K_{rr}/K_{rr})$, weaken with radial distance as $e^{-r/S}$, with $S = 10$ AU, and the rest of the parameters in Eq. (6) independent of r. In Fig. 1a the magnitude of the Fd calculated with the 1D numerical model decreases exponentially with r [see Eq. (7)] and agrees qualitatively with the linear analysis. Quantitatively, the radial dependence of the magnitude of the Fd is considerably larger than predicted by the linear analysis. In Fig. 1b the linear analysis predicts a radially independent recovery time [see Eq. (8)] while the numerical 1D model gives a recovery time that increases

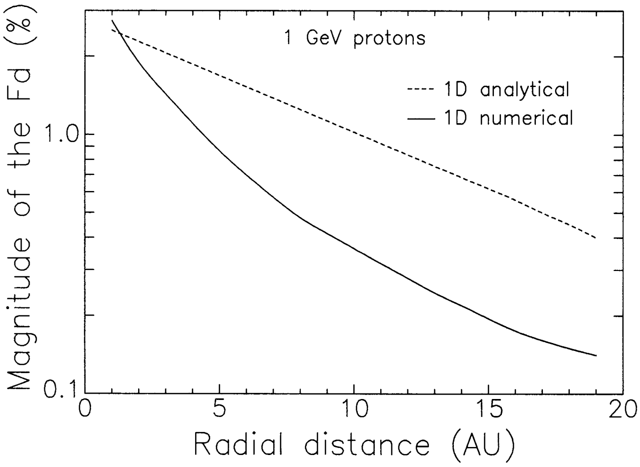

Fig. 1a. The magnitude of the Fd as a function of radial distance. The 1D numerical simulation is compared with 1D analytical results of Chih & Lee (1986). Magnitude is given by $(j_0 - j_1)/j_0$, with j_0 the undisturbed intensity level before passage of disturbance and j_1 the minimum intensity level caused by the propagating disturbance. Amplitude of propagating disturbance decays in both models like $e^{-r/10}$, with r radial distance in AU, and rest of parameters in Eq. (6) independent of r

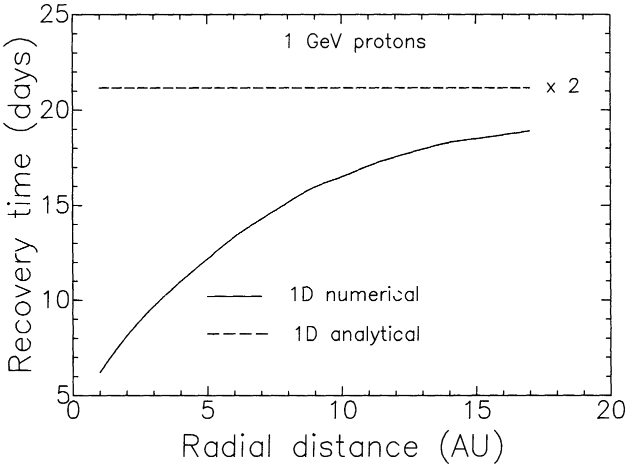

Fig. 1b. The recovery time, t_r, of the Fd shown in Fig. 1a as a function of radial distance; t_r is calculated as the time for Fd to recover to a 1/3 of its maximum decrease. The 1D analytical result must be multiplied by 2 to get actual values

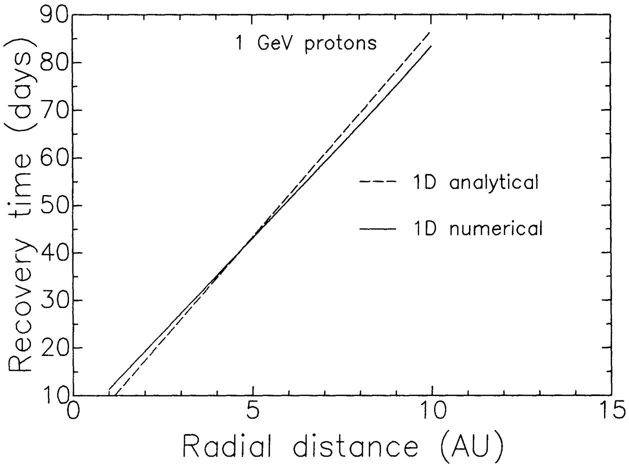

Fig. 2b. The recovery time of the Fd shown as a function of radial distance with models same as in Fig. 2a

sharply with radial distance in the inner heliosphere, but levels off at larger radial distances at much smaller values than given by the linear analysis calculations. The reason for this, and the quantitative differences in Fig. 1a, will be discussed in detail when Fig. 4 is shown.

In Fig. 2a and b, K_{rr} was given a linear radial dependence while the rest of the parameters in Eq. (6) were kept unchanged as in the second example. The magnitude of the Fd, in Fig. 2a, as calculated with our model has a similar radial dependence as the $1/r$ dependence of the linear analysis prediction – see Eq. (9). In Fig. 2b the analytical prediction of a linear radial dependence for the recovery time of the Fd [see Eq. (10)] is also obtained with our model, in fact, the recovery times actually agree remarkably well.

In Fig. 3a the magnitude of the Fd as a function of radial distance with the 1D model is compared with that of the linear analysis with all the parameters in Eq. (6) radially independent as in the third example. Our model calculations show virtually

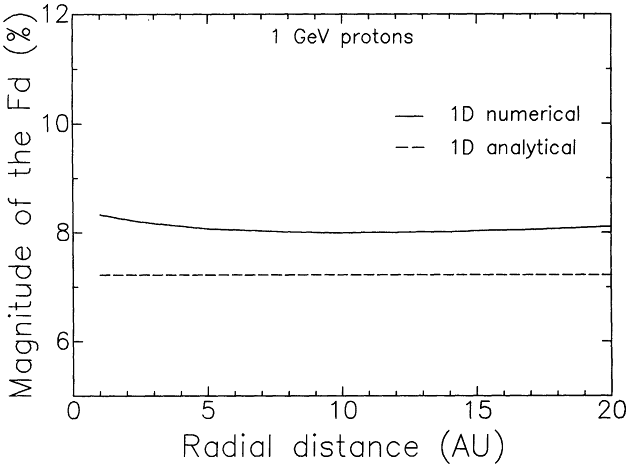

Fig. 3a. The magnitude of the Fd for the 1D numerical model compared with the analytical model. For both models all the parameters in Eq. (6) were specified independent of radial distance

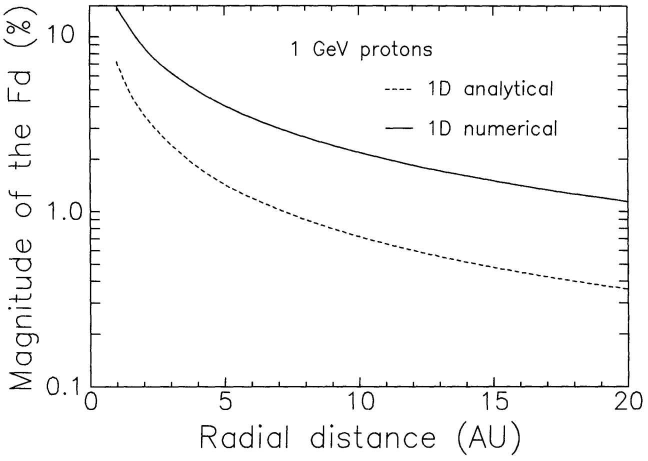

Fig. 2a. The magnitude of the Fd for the 1D numerical model compared with the analytical model as a function of radial distance. In this case $K_{rr} \propto r$ with rest of parameters in Eq. (6) independent of r for both models. The magnitude of the Fd decreases as kr^{-1}, with k a constant, as predicted by linear analysis

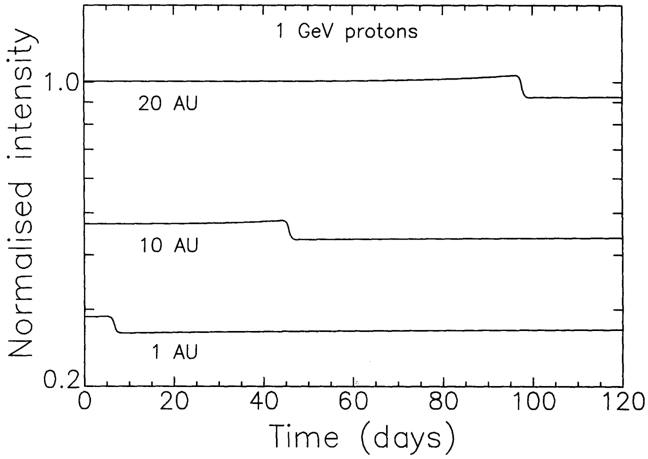

Fig. 3b. The 1D numerical model as in Fig. 3a with intensity-time profile of Fd displayed at three positions in the heliosphere. The Fd does not recover at any radial distance. All intensities normalised to pre-Fd intensity level at 20 AU

no radial dependence in quantitative agreement with the linear analysis. This, of course, shows that the Fd will essentially have the same magnitude throughout the heliosphere. In Fig. 3b we show the intensity as a function of time (i.e., the Fd intensity-time profiles) at three positions in the heliosphere. There is no recovery in the decreased intensity whatsoever at all radial distances in accordance with the prediction of the third example. This points to the fact that so long as the disturbance remains at the same level of efficiency (in keeping out inward diffusing particles) as a function of radial distance, the intensity will not recover behind the disturbance. Qualitatively, therefore, our model is in agreement with the predictions of Eq. (6), except for Fig. 1b.

In Fig. 4 we show the magnitude of the Fd as a function of the amplitude of the disturbance which was varied between 0.23 and 0.9. According to the linear theory the magnitude of the Fd is proportional to the amplitude of the disturbance so that on a logarithmic scale the gradient is 1. For the numerical model the gradient approaches this value only at small amplitudes. Our somewhat more comprehensive model therefore agrees with the linear analysis at small amplitudes which is one of the assumptions upon which the linear analysis was based. At larger amplitudes the gradient becomes increasingly >1 for the numerical model meaning that the magnitude of the Fd becomes more sensitive to changes in the amplitude of the disturbance. This explains the fact that our model gives a much larger radial dependence for the magnitude of the Fd shown in Fig. 1a than predicted by the linear analysis. In that case the amplitude of the disturbance in the inner heliosphere was still large and this is where in Fig. 4 it is proved that the magnitude of the Fd to be the most responsive to changes in the amplitude of the disturbance. This in turn also explains the qualitative difference between our model and the predictions of the linear analysis regarding the recovery times in Fig. 1b. As the disturbance travels radially outwards, its ability of being an effective barrier against radially inward diffusing particles deteriorates faster in our model and so the recovery times, especially in the inner heliosphere, are much shorter than given by the linear theory. *Our model therefore approximates the predictions of the linear theory under the same conditions!*

In Fig. 5 we display the intensity-time profiles of a Fd for 1 GeV protons at two different positions in the equatorial plane;

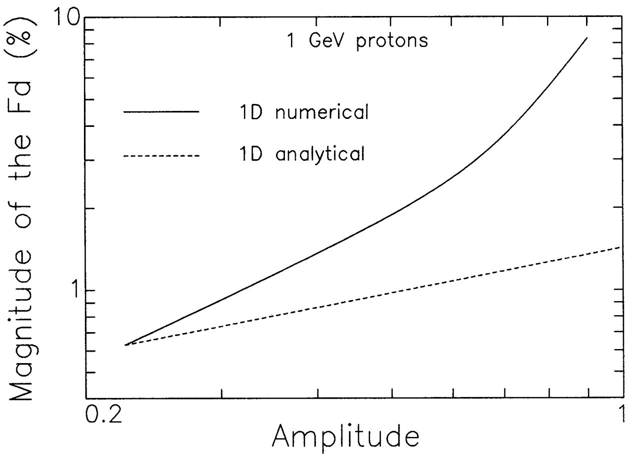

Fig. 4. The magnitude of the Fd shown for both 1D numerical and analytical models with amplitude of disturbance varied from 0.23–0.9

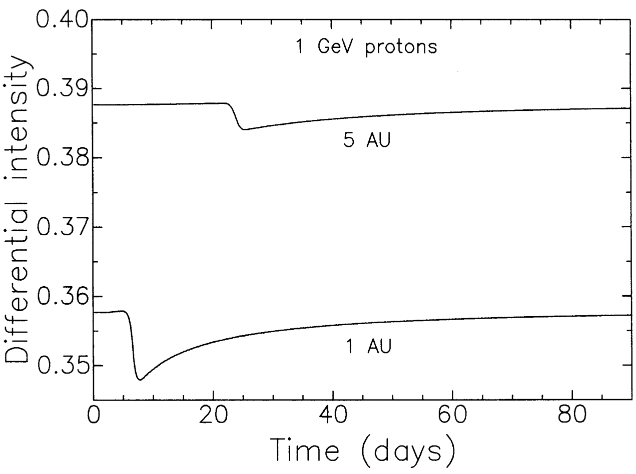

Fig. 5a. The 1D numerical model as in Fig. 1 with the Fd shown on an intensity-time scale at two positions in the heliosphere; differential intensity in units of $m^{-2} s^{-1} sr^{-1} GeV^{-1}$

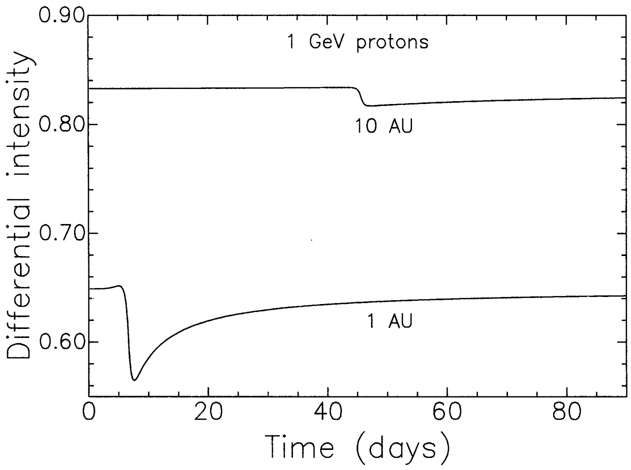

Fig. 5b. Same as Fig. 5a for the 1D numerical model in Fig. 2

in Fig. 5a when the amplitude of the propagating disturbance decays with increasing radial distance as in Fig. 1a and b and in Fig. 5b when the radial diffusion coefficient K_{rr} increases with radial distance as in Fig. 2a and b. In both figures the intensity-time profiles with their small precursors, sharp decreases and exponential recoveries over a few days show strong agreement with the features of observed Fd's. This implies that in order to simulate a Fd realistically in a 1D model it is important that either the disturbance should decay with radial distance (example 1) or that K_{rr} should increase with radial distance (example 2). This is in agreement with the results of Nishida (1982) and Chih & Lee (1986). If neither of the two happens no recovery will occur, as in Fig. 3a and b, so that a realistic intensity-time profile of a Fd can only be simulated when the propagating disturbance somehow becomes less effective in blocking out radially inward diffusing particles with increasing radial distance. Crossfield diffusion of particles around the disturbance does not play any role in the spherically-symmetric modulation process, of course. It must be pointed out that for both Fig. 5a and b there were a decrease in the magnitude and an increase in the recovery time of the Fd with increasing radial distance in qualitative agreement with the observations of Lockwood & Webber (1987) and Webber et al. (1986) and is quite amazing for such a simple model. The radial dependence of the magnitude compared with these observations, however, was too strong because the 1D model predicted a Fd that tended to become extremely small at larger radial distances (Figs. 1a and 2a) while a weak radial dependence for the magnitude was observed by Webber et al. (1986) and Lockwood & Webber (1987). Then, the consequence of simulating a realistic Fd at Earth with a 1D model is that it seems unable to explain this weak radial dependence of the magnitude of the Fd. If it is ensured that the magnitude of the Fd has a small radial dependence (as in Fig. 3a) the characteristic exponential recovery associated with Fd's does not materialise. We therefore disagree with Perko (1987) that a realistic Fd can be simulated in a 1D model with a disturbance which does not decay with radial distance while encountering a radially independent mean free path. It is also interesting to notice in both Fig. 5a and b how the time for the Fd to reach its minimum intensity is predicted to increase with radial distance, qualitatively in agreement with the observations of Webber et al. (1986).

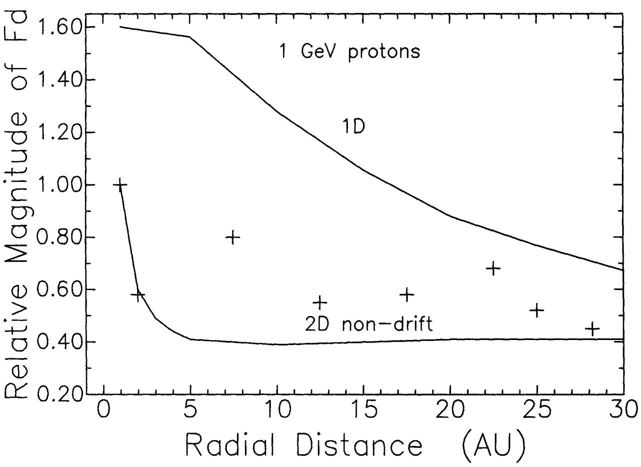

Fig. 6a. Magnitude of the Fd relative to its value at 1 AU for the 1D numerical model and the 2D non-drift model. The + symbols portray data from Webber et al. (1986)

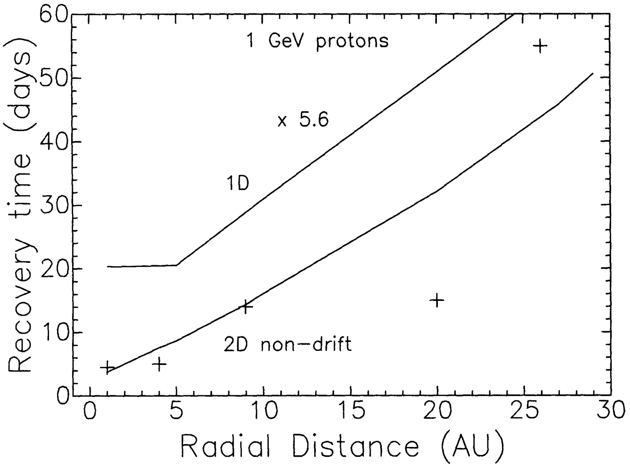

Fig. 6b. The recovery times for the 1D and 2D non-drift models shown in Fig. 6a. Data are from Webber et al. (1986). Values for the 1D model must be multiplied by 5.6 to get actual values

4. The simulation of Fd's with an axially-symmetric non-drift model

Before introducing the additional complication of drift in the large scale IMF in our model it is useful to look at the role of diffusion perpendicular ($K_\perp$) to the IMF as well the latitudinal extent of the disturbance in determining the recovery and decrease caused by a travelling disturbance. In this version the only simplification therefore is that the drift associated coefficients $K_{r\theta}$ and $K_{\theta r}$ are neglected in the computer code.

In the next two figures a direct comparison is made between the spherically-symmetric and the current model with respect to the magnitude and the recovery time of the Fd for 1 GeV protons in the equatorial plane. These calculations are also compared with the experimental data of Webber et al. (1986) as a function of radial distance in the equatorial plane. To do the comparison between the two models it was ensured that the radial diffusion and the solar wind velocity were the same in the equatorial plane for both models. For the 2D model the latitudinal extent of the disturbance was fixed at 15° above and below the equatorial plane and $K_\perp = 0.05 K_\parallel$. A value of 3.4 was specified for K_0 in Eq. (2a) which corresponded to solar minimum conditions. *The disturbance was allowed to propagate without any radial evolution or merging with other disturbances.* In Fig. 6a the magnitude of the Fd as a function of radial distance for both the 1D model and 2D non-drift model is shown. The model calculations and the experimental data were normalised at 1 AU. Here, one can see that the magnitude of the Fd calculated with the 2D model shows a steep decrease at smaller radial distances, but is nearly independent of radial distance further out. This steep decrease is primarily the consequence of assuming $K_\parallel \propto K_\perp \propto 1/B$ and can therefore be restrained, if required, by using a different spatial dependence for $K_\parallel$ and for $K_\perp$ [Eq. (2a) and (2b)]. The magnitude of the Fd with the 2D model is significantly smaller compared with that of the 1D model, especially at smaller radial distances, and can be understood "semi-quantitatively" by using a simple linear combination of $K_\parallel$ and $K_\perp$ based on the ratio of the components of the differential diffusion stream in the TPQ: The magnitude of the Fd in the 1D model is, according to Eq. (6), proportional to $(1/K_{rr})$ at any specified radial position [with all the other parameters in (6) fixed], but with the 2D model

$$(\Delta j_T/j_T)_{\max} \propto 1/K_{rr} - K_\perp/rK_\parallel \, . \tag{11}$$

Since this model produces a latitudinal gradient (following from the spatial dependence of the diffusion coefficients which ensures that they are larger at higher latitudes), particles at higher latitudes diffuse inwards to the Sun but also downwards to lower latitudes because of crossfield diffusion. The travelling disturbance, acting as a semi-penetrable barrier to inward diffusing particles, now also has to deal with the extra contributions from higher latitudes and is therefore less successful in sweeping away the incoming particles causing smaller decreases compared with those of the 1D model as shown in Fig. 6a. According to the data in this figure the magnitude of the Fd has a moderate radial dependence in the equatorial plane and in that aspect agrees well with the 2D model except for very small radial distances. The 1D model is obviously less successful. In Fig. 6b the recovery times of the Fd for the two models are shown as a function of radial distance in the equatorial plane. The 2D result shows an almost linear increase with radial distance and is significantly less than for the 1D model. With the additional complexities of latitudinally dependent modulation, in terms of diffusion and solar wind velocity, a simple expression like Eq. (11) can, unfortunately, not be used, not even qualitatively, to predict these tendencies in the recovery times correctly. However, the principle stated in the previous section that the recovery time is determined by what modulation conditions the propagating disturbance encounters between the observer and the modulation boundary, and not by the local values of the parameters, can still be applied to explain this significant reduction in the recovery times. For instance, in the 1D version the only way the intensity can recover behind the disturbance is through the radially inward diffusion of cosmic rays through the moving disturbance, provided that the effectiveness of the disturbance in forming a barrier against cosmic rays grows less while propagating radially outwards as illustrated in Figs. 1a and 2a. In the axially-symmetric model diffusion perpendicular to the IMF occurs and plays an important role. We specified the latitudinal extent of the disturbance at 15° above and below the equatorial plane which allowed particles to diffuse freely around the disturbance to fill up the cavity left behind by the disturbance. In other words, the recovery time of a Fd, at a particular position, according to the 2D model depends not only on the decrease in the effectiveness of the disturbance to sweep away incoming particles with radial distance, but is also strongly influenced by the latitudinal extent of the disturbance combined with the effect of $K_\perp$. (This will be illustrated in detail in Figs. 8 and 9.) The full impact of latitudinal diffusion is, of course, determined by the latitudinal dependence of the diffusion coefficients used. This latitudinal dependence (e.g., $K_{rr} \propto r^2$ at $\theta = 0°$, but only $\propto r^{0.5}$ at $\theta = 90°$) ensures that the latitudinal gradient is large enough to make diffusion in the latitudinal direction quite effective. How large this off-equatorial contributions in reality are is unknown due to the lack of observations at higher latitudes. The *increase in the recovery time with radial distance is*, however, not only determined by the specified spatial dependence of the diffusion coefficients, but also by the developing geometry of the propagating disturbance as were established with several test runs. Although the disturbance has a fixed radial and latitudinal extent at all radial distances, it acquires an area which increases proportional to r in our spherical coordinate system and so becomes a more effective barrier against incoming particles at larger radical distances. This view was in fact also proposed by Webber et al. (1986) as an explanation for the increase in the recovery times observed for the Fd as a function of radial distance shown in Fig. 6b. In that figure the recovery times with the 2D model are compatible with the data, but in contrast to the much too long recovery times of the 1D model. The reasonable compatibility of 2D results with the data concerning both the magnitude and the recovery time of the Fd in the equatorial plane emphasises the important role of perpendicular diffusion and the latitudinal extent of the propagating disturbance if realistic simulations of Fd's are to be done. The fact that this compatibility with the data (observed during periods of increased solar activity from 1978–1984) has been achieved with an isolated propagating disturbance might imply that such disturbances, causing Fd's, could also be present during these more active periods *or* that an isolated propagating disturbance could produce for the magnitude and the recovery time a radial dependence for Fd's similar to those observed between 1978–1984 when merging effects were supposedly more important.

In Fig. 7a and b respectively we show the corresponding intensity-time profiles *at Earth* of Fd's simulated with the 1D and the 2D models of Fig. 6. These profiles are normalised to the undisturbed pre-Fd intensity levels. Shown in Fig. 7a is the fact that the combination of a disturbance without radial evolution and a K_{rr} in the equatorial plane with a weak radial dependence ($K_{rr} \propto r^{0.5}$) produces, in the case of the 1D model, an unrealistic Fd because of its very slow recovery of 111 days while the 2D model, on the other hand, gives a very realistic time-profile for the Fd and also features quite prominently at larger radial distances as shown in Fig. 6. In Fig. 7c we also show the intensity-time profile of the Fd with the 2D model at 20 AU, normalised to the intensity-time profile in Fig. 7b. From 1 AU to 20 AU the magnitude of the Fd decreases from 9% to 4%, while the recovery time increases from 4 days to 33 days in accordance with what was shown in Fig. 6. A surprising aspect of the Fd at 20 AU is the extraordinary large precursor compared with what was found at 1 AU. It is, of course, to be expected that the model which is based on simplified modulation conditions (e.g., neglecting azimuthal effects) will produce larger precursors than what follows from observations. Nevertheless, this prediction seems in qualitative agreement with observations reported by McDonald et al.

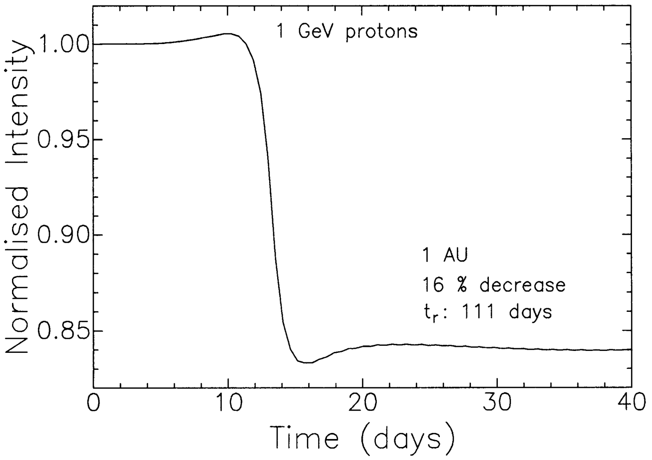

Fig. 7a. The Fd shown at Earth on an intensity-time scale for the 1D model in Fig. 6

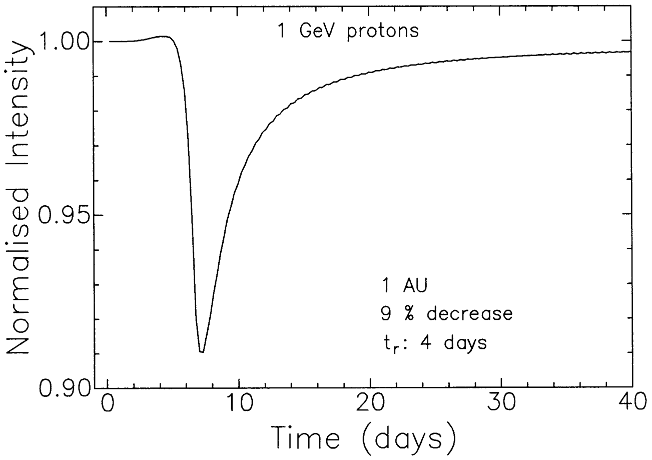

Fig. 7b. Same as in Fig. 7a with the 2D non-drift model

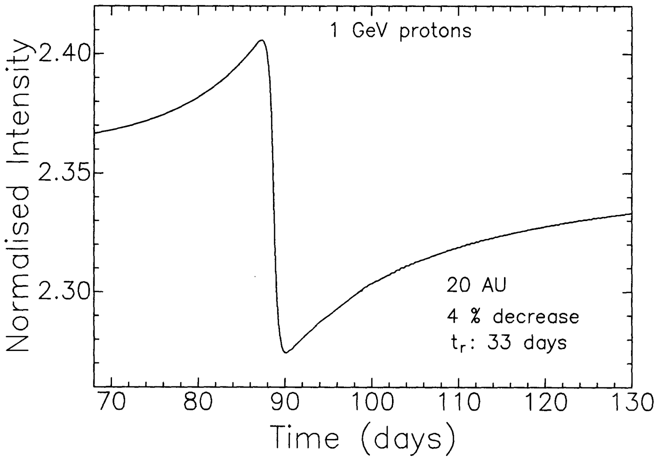

Fig. 7c. Same as in Fig. 7b, at 20 AU. Intensity is normalised to the pre-Fd intensity level of Fig. 7b

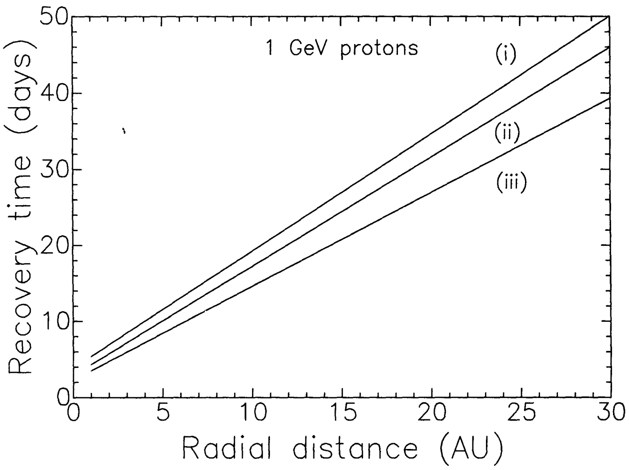

Fig. 8b. The recovery times of the Fd for the respective values of $K_\perp$ in Fig. 8a

(1981). This feature will be discussed further when the results of a drift model are shown.

In the absence of any analytical 2D work we will illustrate with the next four figures what the effects of $K_\perp$ and the latitudinal extent of the disturbance are on the recovery times and magnitude of Fd's. The results of these Figures are comparable to those of Thomas & Gall (1984) who followed a totally different approach by applying Monte Carlo techniques. In Fig. 8a and b the magnitude and recovery time of the Fd as a function of radial distance in the equatorial plane for 1 GeV protons are shown respectively. The calculations were done with $K_\perp = 0.025K_\parallel$; $0.05K_\parallel$, and $0.1K_\parallel$ and illustrate that the magnitude of the Fd becomes smaller at almost all radial distances when $K_\perp$ is increased, and is qualitatively in accordance with Eq. (11). The increase in $K_\perp$ results in an increase in the radial dependence and magnitude of K_{rr} so that stronger radial diffusion as well as perpendicular diffusion occur. The propagating disturbance is consequently less effective in barring incoming particles and the magnitude of the Fd is reduced. In Fig. 8b one can see that recovery time is also reduced at all radial distances in the equatorial plane when $K_\perp$ is increased. This increase in $K_\perp$ allows particles to diffuse more freely around the disturbance and causes therefore an increase in the tempo with which the cavity, left behind by the propagating disturbance, will be filled. The increased radial dependence of K_{rr} when $K_\perp$ is increased now causes the effectiveness of the disturbance in forming a barrier against incoming cosmic rays to increase at a slower rate while propagating radially outwards and thereby also contributes to the reduced recovery times.

Figure 9a and b show respectively what happens to the magnitude and the recovery time of a Fd in the equatorial plane when the latitudinal extent of the disturbance in increased from 6° to 15°, and then for illustrative purposes to the extreme of 90°, above and below the equatorial plane. According to Fig. 9a the latitudinal expansion of the disturbance results in an increase in the magnitude of the Fd at all radial distances as well as an increase in the radial dependence of the magnitude in the equatorial plane, especially at smaller radial distances. This reflects the fact that a larger latitudinal extent for the disturbance enhances the ability of the propagating disturbance to act as an effective barrier against incoming particles. In Fig. 9b a larger latitudinal extent for the disturbance results in a significant increase in the recovery time of the Fd at all radial distances. At higher latitudes more

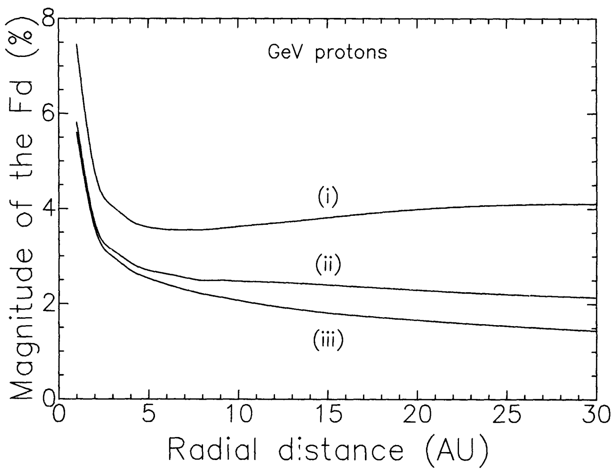

Fig. 8a. The magnitude of the Fd, as a function of radial distance, calculated with the 2D non-drift model for: (i) $K_\perp = 0.025K_\parallel$, (ii) $K_\perp = 0.05K_\parallel$ and (iii) $K_\perp = 0.1K_\parallel$

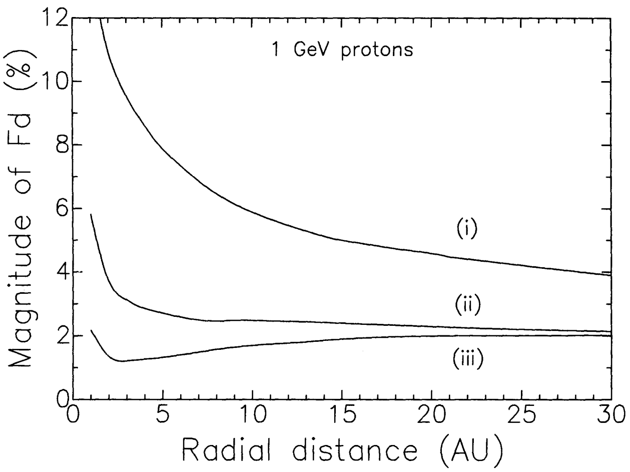

Fig. 9a. The magnitude of the Fd calculated with the 2D non-drift model for different values of the latitudinal extent of the disturbance above and below the equatorial plane: (i) 90°, (ii) 15° and (iii) 6°

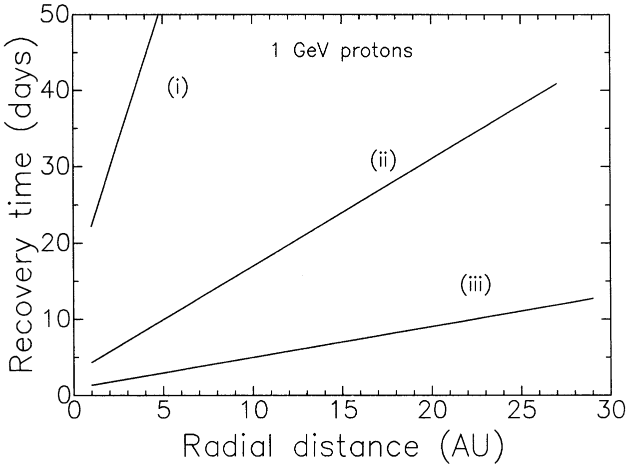

Fig. 9b. The recovery times of the Fd with the parameters of Fig. 9a

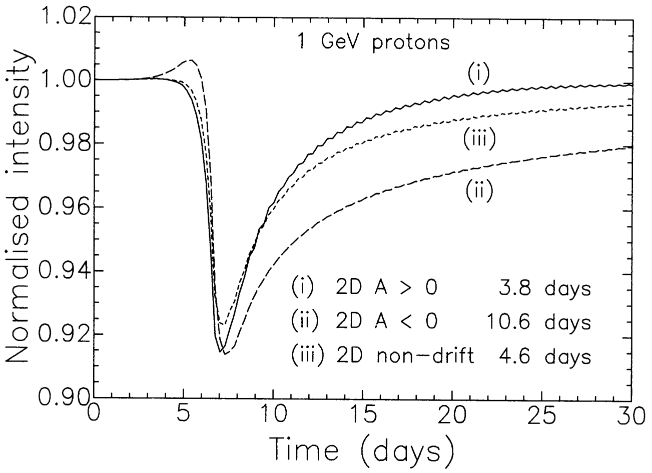

Fig. 10. Intensity-time profiles with the recovery times of the Fd at Earth for the 2D drift model ($A > 0$ and $A < 0$), and the 2D non-drift model. A neutral sheet tilt angle of 10° was used for the drift model. (The small wiggles are artificial and result from the used grid.)

particles are barred from diffusing around the larger disturbance and so the recovery rate of the decreased intensity behind the disturbance is retarded to become unrealistically large when 90° is used. An interesting aspect to note from Fig. 9a and b is how the increase in the latitudinal extent of the disturbance leads to results which become quantitatively similar to that of the 1D model shown in Fig. 6a and b. These geometrical effects can be attributed to the fact that the 2D disturbance, when enlarged to be present at all latitudes (latitudinal extent of 90°), actually becomes a barrier which surrounds the Sun at all latitudes producing effects similar to that of the 1D model.

5. The simulation of Fd's with an axially-symmetric drift model

In this section we study the decrease and recovery of Fd's with a 2D model which includes gradient and curvature drift as well as a simulated wavy neutral sheet. This leads, of course, to a scenario for heliospheric modulation that is considerably more complex and little success is achieved with any attempt to describe the characteristics of the Fd by a simple linear combination of diffusion coefficients as in Eq. (11), for instance. In order to gain some understanding of the effects of drift and the neutral sheet we compare results when $A > 0$ (northern-hemispheric IMF points away from the Sun) with when $A < 0$ (northern-hemispheric IMF points towards the Sun) and for increased waviness of the neutral sheet. This enables us to present novel results which predict how the recovery times will be effected by different tilt values of the neutral sheet and by the polarity reversal of the IMF. These predictions can then be used to evaluate the role of drift on Fd's in the heliosphere.

In Fig. 10 we show simulated intensity-time profiles for Fd's done for 1 GeV protons at Earth respectively for the epochs with $A > 0$ and $A < 0$, and also when drift effects were neglected. The drift cases were done with a neutral sheet tilt angle, $\alpha = 10°$, which represents solar minimum conditions, and $(K_T)_0 = 1$ in Eq. (3). The rest of the modulation parameters were kept as specified for the 2D non-drift model in the previous section. It is shown in this figure that the characteristics of a typical Fd at 1 AU, namely a small precursor (but only for $A < 0$), a fast decrease and more gradual almost exponential recovery of a few days are present. The recovery times show a marked change when the polarity of the IMF is reversed – it changes from ~ 3.8 d when $A > 0$ to ~ 10.6 d when $A < 0$. The non-drift result lies in between with a recovery time of ~ 4.6 d. These tendencies agree with the results of Kadokura & Nishida (1986). A very interesting prediction of our model is that precursors should occur more frequently during $A < 0$ epochs because of the peculiar drift velocity field in conjunction with diffusion during those periods.

The results shown in Fig. 10 can easily be explained by considering the direction of particle drift in the heliosphere. During an $A > 0$ epoch positive particles drift from high heliospheric latitudes down towards the equatorial plane and outwards along the neutral sheet. Drift and diffusion are then complementing each other at higher latitudes, while in the equatorial regions drift and the radially inward directed diffusion are in opposition. Under these circumstances the cavity left behind by the propagating disturbance in the equatorial regions will be filled at a more rapid rate when $A > 0$ than with drift neglected. Neutral sheet drift and radial diffusion are complementing each other in the equatorial regions, when $A < 0$, but the particles also drift away from the equatorial plane so that the filling in of the cavity by particles scattering through the disturbance and latitudinally around is less effective than when they drift downwards from the polar regions. The recovery rate with $A < 0$ is consequently slower than in the non-drift case, and even more so when $A > 0$. The response of the magnitude of the Fd to the polarity change of the IMF is however small, illustrating that drift has an almost negligible effect on the magnitude of Fd's *at Earth.* At larger radial distances, however, the effect of drift on the magnitude and the recovery time of the Fd actually increases and will be discussed in more detail when Fig. 12 is shown. Despite the complexity of a drift description of modulation it was found that the importance of drift as judged by the magnitude of the polarity-reversal effect can qualitatively be explained by considering the radial dependence of K_T in the equatorial plane [$K_T \propto r$; Eq. (3)], which is according to our assumption the result of the radial dependence of the Parker spiral field. Since K_T is smaller at small radial distances it produces less pronounced drift effects at Earth compared with larger radial distances so that the polarity reversal of the IMF should be less able to effect the magnitude of the Fd at Earth.

Observationally, Lockwood et al. (1986) found an average recovery time of about 5 days for Fd's at 1 AU which compares remarkably well with the model's predictions for the non-drift and $A > 0$ drift case. For $A < 0$ the predicted recovery time of 10.6 days is much longer than observed, of course. In fact, this large effect of the polarity reversal of the IMF has not been observed, although some, but barely statistically significant drift effects were reported by Mulder & Moraal (1986). One should keep in mind, however, that the results shown in Fig. 10 were obtained with $\alpha = 10°$, i.e., for minimum solar activity. Since many of the Fd's in the above-mentioned data analyses were actually observed during times of increased solar activity, the question arises what effect an increasing α would have on the recovery times before and after the reversal of the polarity of the IMF. This is demonstrated in Fig. 11 where the recovery times of Fd's at Earth for 1 GeV protons are plotted as a function of increasing diffusion for the two polarity epochs for the IMF, for periods of low and high solar activity, i.e., tilt values of 10° and 50° respectively, and compared with the recovery times for the non-drift case. From this figure it follows that: (1) The recovery time is more sensitive to changes in the waviness of the neutral sheet when $A < 0$. This makes sense because when $A > 0$ the emphasis is more on a recovery with particles coming from higher latitudes where the neutral sheet is relatively unimportant whereas when $A < 0$ particles primarily encounter the disturbance head on, and the effect of the changing waviness of the neutral sheet becomes important. (2) The effect of the polarity change is smaller with large tilt values – the recovery times are generally smaller for large tilt values when $A < 0$, but somewhat larger when $A > 0$. (3) The effect of a polarity reversal on the recovery time is also dependent on the amount of diffusion since the recovery times seem to converge with the non-drift case with increasing diffusion, illustrating how drift loses ground against the stronger diffusion. With little diffusion, changes in the waviness of the neutral sheet actually become ineffective when $A < 0$, suggesting that drift is so dominant that not even a factor of 5 change in the waviness of the neutral sheet can influence the recovery rate. These results indicate that drift effects on the recovery times of Fd's are at its largest when the tilt angle of the neutral sheet is small, and that the drift effect must preferably not entirely be judged by a data analysis of Fd's over all degrees of waviness as had been done (Lockwood et al. 1986; Mulder & Moraal 1986; Morishita et al. 1990).

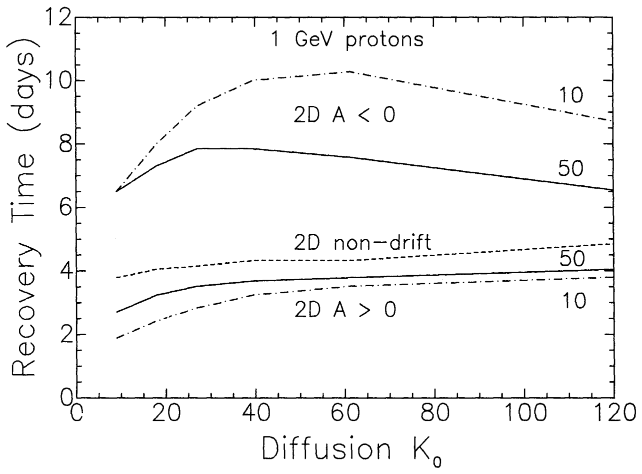

Fig. 11. Recovery times of Fd's at Earth as a function of increasing diffusion for the drift model with $A > 0$, $A < 0$, $\alpha = 10°$ and 50°, and no drift respectively. K_0 in units of $6\,10^{20}\,\mathrm{cm^2\,s^{-1}}$ – see Eq. (2a)

Although the maximum polarity-reversal effect of the IMF on the recovery time at Earth shown in Fig. 11 is reduced significantly from ~6.5 day difference, with small tilt values, to ~4 day difference, with large tilt values, when the polarity of the IMF is changed, the difference of 4 days is still large compared with the almost negligible observed effect. We subsequently considered three other variations of our model. First, the suggestion of Jokipii & Kóta (1989) that the solar polar field has a transverse component which becomes important at larger radial distances and deviates from the generally accepted Parker spiral field in those regions which should lead to decreased drift effects, especially when $A > 0$. Using this approach we altered the field magnitude substantially in the polar regions – by a factor 40 at $\theta = 0°$, when $r = 40$ AU, but only a factor 1.2 in the equatorial plane at $\theta = 90°$. The effect on the recovery times at Earth is shown in Table 1 compared with that for the standard spiral field approach. Evidently, the polarity-reversal effect on the recovery times remains as strong as before, although the recovery times differ from the standard spiral field values. The reason is that the new solar polar field deviates very little from the Parker spiral field in the inner heliosphere, implying that the reduction should be larger at larger radial distances. Secondly, following Lockwood et al. (1986), we used a propagating disturbance which decayed exponentially like $e^{-r/7}$. It follows from Table 1 that this approach significantly increased the recovery rate when $A < 0$, and thereby reduced the polarity-reversal effect remarkably. The reason is that a decaying barrier is less effective stopping particles drifting inward along the neutral sheet. Although more successful in explaining the observed small polarity-reversal effect on the recovery times the decay of disturbances means that Fd's will tend to die out at larger radial distances which seems contrary to the results of Lockwood & Webber (1987). Furthermore, according to Burlaga et al. (1985) disturbances seem to merge producing large MIR's which should have a profound effect on the modulation. Experimental results therefore support, in general, stronger effects with increasing radial distance rather than decaying effects. The third explored option is the argument that drift was generally too strong and had to be scaled down as originally proposed by Potgieter et al. (1989). In conjunction, Webber at al. (1990) found that it was necessary to reduce drift by a factor of 2 at lower energies, $E = 120$–227 MeV, in their steady state drift model in order to achieve a good correlation between their predictions and data when $A < 0$ (1980–1987) and $\alpha \gtrsim 35°$. Furthermore, Le Roux & Potgieter (1990a) – see also Potgieter & Le Roux (1990) – showed that a time-dependent drift

Table 1. Effect of four different approaches on the recovery times of Fd's. Normalised values are given in parentheses

Approach	Recovery time (days) at Earth	
	$A > 0$	$A < 0$
Parker spiral field (standard)	3.8 (1.0)	10.6 (2.8)
Solar polar field deviation	4.9 (1.0)	13.3 (2.7)
Equatorial disturbance decay	3.5 (1.0)	6.0 (1.7)
Drift reduced by a factor of 3	4.3 (1.0)	6.5 (1.5)

model with real neutral sheet values incorporated was generally successful in explaining the observed intensity-tilt relationship for $E \geq 60$ MeV protons from 1976–1987 only when $\alpha \leq (35 \pm 5)°$. The intensity-tilt correlation with the data also showed a too large drift effect when the polarity of the IMF was switched. Decreased drift is also supported by the observation that the IMF had increased from ~5 nT in 1976 to ~9 nT in 1982 (Winterhalter et al. 1990). Since it is generally assumed that $K_T \alpha 1/B$ this observation implies that drift would decrease by a factor of almost 2 with increasing solar activity. A too large drift effect with an IMF polarity reversal was also found by Potgieter & Burger (1990) when they studied the He/($e^+ + e^-$) ratio with a steady state drift model for particles with a rigidity of 800 MV. An overall reduction of drift by at least a factor of 2 was needed to predict a ratio compatible with observations. From these references and present results follow that from both a theoretical and observational viewpoint there is ample evidence in favour of decreased drift. To study the effect of such a reduction we scaled drift down by a factor of 3 [$(K_T)_0 = 0.33$ in Eq. (3)]. The result is presented in Table 1 and shows that the recovery time at Earth increased by 2.2 days when the polarity of the IMF was changed. Although this change at Earth is more reasonable the situation at larger radial distances in the equatorial plane is different. For example, in Fig. 12a the magnitude of the Fd as a function of radial distance in the equatorial plane, for both polarities of the IMF and with drift scaled down by a factor of 3, is compared with that of the 2D non-drift model and illustrates that although the magnitude of the Fd is quite similar in the inner heliosphere, the difference for the two polarity epochs increases with radial distance. A similar pattern is noticeable in the recovery times shown in Fig. 12b – for the drift model they deviate increasingly from each other and from the non-drift model with increasing radial distances. (As mentioned before, this increase in the polarity-reversal effect on both the magnitude and the recovery time of the Fd at larger radial distances can be related to the radial dependence of K_T in the equatorial plane.) This, incidentally, provides another way of evaluating the role of drift with regard to Fd's. *If drift is important*, observations should reveal an increase in the effect of the polarity change of the IMF on the magnitude, but especially the recovery times, of Fd's with increasing radial distance.

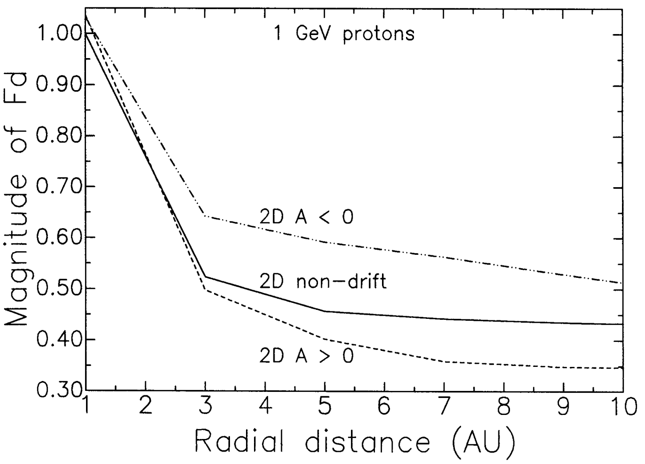

Fig. 12a. The magnitude of Fd's simulated with the 2D drift model when drift is reduced by a factor of 3. The 2D non-drift result is shown for comparison. Values are normalised to those of the non-drift model at 1 AU

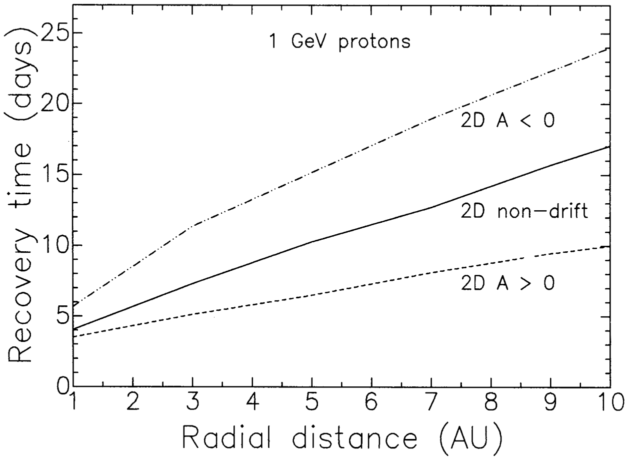

Fig. 12b. Same as in Fig. 12a, with the recovery times of the simulated Fd's

Decreased drift effects nonetheless give a radial dependence for these quantities which is much closer to that of the non-drift model than what would have been the case for full drift. Since we have shown in Fig. 6a and b that the 2D non-drift model gives reasonable compatibility with data, the option of decreased drift has an advantage over the previously discussed option of a decaying travelling disturbance. The reason is that decreased drift not only has the potential of resolving the problem of the too large polarity-reversal effect of the IMF on the recovery time at Earth, but also give a reasonable radial dependence for both the magnitude and the recovery time which is not possible with a decaying propagating disturbance.

6. Summary and conclusions

We developed an axially-symmetric time-dependent drift model with a simulated wavy neutral sheet with which Fd's were modelled by assuming that they were caused by propagating regions of enhanced scattering and diminished drift. We subsequently studied the magnitude of the Fd and its recovery time as a function of radial distance in the equatorial plane. The model was first simplified into a 1D model to be tested against the results of the linear analysis of Chih & Lee (1986). From the linear analysis it firstly followed that in our numerical 1D model version the magnitude of a Fd at a particular position in the heliosphere should be determined by Eq. (6). Second, the magnitude of the decrease was determined by the local modulation conditions, i.e., the solar wind velocity and the radial diffusion coefficient, and characteristics of the disturbance, i.e., the radial extent and the amplitude. This is to be contrasted with the recovery, which, in being less abrupt then the decrease, was determined by the modulation conditions which the propagating disturbance encountered and the evolution of the disturbance during propagation between the observer and the modulation boundary. Overall, the 1D numerical model behaved qualitatively in accordance with the results of the linear analysis. Quantitative differences were found to be the result of the assumptions upon which the linear analysis rested like small perturbations and the neglect of energy changes. To simulate a realistic Fd at Earth with the 1D model it was necessary to use a disturbance that became less effective in sweeping away inward diffusing particles at larger radial distances as it travelled radially outwards either by: (1) the decay of the amplitude or the radial dimension of the disturbance; (2) or an increase in the radial dependence of K_{rr}. In both cases we found a decrease in the magnitude of the Fd and an increase in the recovery time with increasing radial distance which corresponded qualitatively with observations (Webber et al. 1986; Lockwood & Webber 1987). The radial dependence of the magnitude, however, was too strong with the result that the 1D model predicted that the Fd could only barely reach large radial distances in the heliosphere and, if so, in a much reduced state contrary to observations.

Applications of the 2D non-drift model showed that the magnitude of Fd adhered qualitatively to the local value of a linear combination of radial and latitudinal diffusion given by Eq. (11). The complexity of a 2D model of the heliosphere, however, did not allow the application of this simple expression to describe the recovery time. The radial dependence of both the magnitude and the recovery time of the Fd showed a promising compatibility with the data of Webber et al. (1986), thereby solving the problem of the vanishing Fd at larger radial distances obtained with the 1D model. This improvement was a natural consequence of the important role of crossfield diffusion and the 2D geometry of the disturbance. The 2D model also predicted an increase in the recovery times of Fd's with radial distance in general agreement with the observations of Webber et al. (1986). This increase in the recovery time was not only determined by the specified spatial dependence of the diffusion coefficients, but also by the developing geometry of the propagating disturbance. Although the disturbance had a fixed radial and latitudinal extent at all radial distances, it acquired an area which increased linearly with increasing radial distance in our spherical coordinate system and so became a more effective barrier against incoming particles at larger radial distances.

The 2D drift model was remarkably successful in giving a realistic intensity-time profile for the Fd at Earth considering the additional complexity brought about by incorporating drift in the model. Little success, however, was achieved with any attempt to describe the characteristics of the Fd with a simple linear combination of diffusion and drift coefficients. The calculated recovery times of Fd's at Earth, however, were noticeably longer during the $A < 0$ epoch (northern hemispheric IMF points towards the Sun) compared with the $A > 0$ epoch (northern hemispheric IMF points away from the Sun) for a small neutral sheet tilt angle, $\alpha = 10°$, which corresponds to solar minimum conditions. This polarity-reversal effect of the IMF was found too large compared with observations (e.g., Lockwood et al. 1986). The drift model also predicted that precursors should appear more frequently during periods when $A < 0$ (e.g., after 1980). We utilised the ability of our model to simulate the effect of the waviness of the neutral sheet on cosmic rays for differing degrees of α to illustrate the resulting change in the polarity-reversal effect as a function of diffusion. We showed for the first time that the polarity-reversal effect was reduced significantly when the tilt angle was increased corresponding to solar maximum conditions. The model clearly predicts that if drift does indeed play a role in modulation, the effect of the polarity reversal of the IMF on the recovery time of Fd's should be noticeable in the data, at least, at or near solar minimum activity and that the effects may be smoothed out if Fd's were studied over an entire solar cycle. Although large tilt values helped to decrease the polarity-reversal effect of the IMF on the recovery time significantly, the effect was still too large. In an attempt to solve the problem we also considered three modifications to the drift model namely the effect of a solar polar field deviating from a Parker spiral field, decaying disturbances as a function of r, and reduced drift (factor of 3). The best results compared with observations at Earth were achieved with reduced drift. The polarity-reversal effect, however, was stronger at large radial distances in the equatorial plane, even for reduced drift. This incidentally provides another way in which the role of drift can be tested if enough data on Fd's become available for two consecutive solar cycles. This apparent necessity for reduced drift may be seen as another argument in favour of the viewpoint that drift effects are generally predicted too large by current models (Potgieter et al. 1989; Webber et al. 1990; Potgieter & Burger 1990; Le Roux & Potgieter 1990a, 1990b; Potgieter & Le Roux 1990). Yet, it must also be remembered that this 2D model of the Fd is a highly idealised simulation simply based on enhanced diffusion and reduced drift. Furthermore, longitudinal modulation which could contribute to a decrease in the polarity-reversal effect on both the recovery times and the precursors of Fd's at Earth had not been addressed. Such effects, however, entail the development of a three dimensional time-dependent code which requires a vast increase in computer time not available to us at this stage. A detailed modelling of the spatial and temporal variation in the solar wind velocity and the IMF in the propagating disturbance have for the same reason also not been attempted. It therefore may well be that a more detailed simulation of the propagating disturbance causing Fd's in both a two- and three-dimensional model could render the reduction of drift for a further improvement in the correlation with data before and after the polarity reversal to be less important. An interesting effect like the influence of the acceleration of cosmic rays at the disturbance on the Fd can also be studied but is only of secondary importance at relative high particle energies, such as 1 GeV, studied in this paper.

Acknowledgements. JAleR thanks Prof. P.H. Stoker for the financial support during 1990. We thank Mrs. P. Sieberhagen for her administrative assistance and Mr. B. Venter for assisting in preparing the figures.

References

Badruddin, Yadav R.S., 1986, Solar Phys. 105, 413
Burger R.A., Potgieter M.S., 1989, ApJ 339, 501
Burlaga L.F., McDonald F.B., Goldstein M.L., Lazarus A.J., 1985, J. Geophys. Res. 90, 12 027
Chih P.P., Lee M.A., 1986, J. Geophys. Res. 91, 2903
Fisk L.A., 1976, J. Geophys. Res. 81, 4646
Jokipii J.R., Kota J., 1989, Geophys. Res. Lett. 16, 1
Kadokura A., Nishida A., 1986, J. Geophys. Res. 91, 13
Laster H., Lenchek A.M., Singer S.F., 1962, J. Geophys. Res. 67, 2639
Le Roux J.A., Potgieter M.S., 1989, Adv. Space Res. 9 (4), 225
Le Roux J.A., Potgieter M.S., 1990a, Proc. 21st Intern. Cosmic Ray Conf., Adelaide, 6, 87
Le Roux J.A., Potgieter M.S., 1990b, ApJ 361, 275
Lockwood J.A., 1960, J. Geophys. Res. 65, 19
Lockwood J.A., Webber W.R., Jokipii J.R., 1986, J. Geophys. Res. 91, 2851
Lockwood J.A., Webber W.R., 1987, Proc. 20th Internat. Cosmic Ray Conf., Moscow, 3, 283

McDonald F.B., Trainor J.H., Webber W.R., 1981, Proc. 17th Internat. Cosmic Ray Conf., Paris, 10, 147
Morishita I., Nagashima K., Sakakibara S., Munakata K., 1990, Proc. 21st Intern. Cosmic Ray Conf., Adelaide, 6, 217
Morrison P., 1956, Phys. Rev. 101, 1347
Mulder M.S., Moraal H., 1986, ApJ 303, L75
Nishida A., 1982, J. Geophys. Res. 87, 6003
Parker, E.N., 1963, in: Interplanetary Dynamical Processes, Interscience Publ., New York
Parker E.N., 1965, Planet. Space Sci. 13, 9
Perko J.S., 1987, J. Geophys. Res. 92, 8502
Potgieter, M.S., 1984, PhD. Thesis, Potchefstroom University for CHE, South Africa
Potgieter M.S., Burger R.A., 1990, A&A 233, 598
Potgieter M.S., Le Roux J.A., 1990, Proc. 21st Intern. Cosmic Ray Conf., Adelaide, 6, 91
Potgieter M.S., Le Roux J.A., Burger R.A., 1989, J. Geophys. Res. 94, 2323
Potgieter M.S., Moraal H., 1985, ApJ 294, 425
Sarris, E.T., Dodopoulos C., Venkatesen D., 1989, Solar Phys. 120, 153
Singer S.F., 1958, Nuovo Cimento, Suppl. Ser. X 8, 334
Thomas B.T., Gall R., 1984, J. Geophys. Res. 89, 2991
Van Allen J.A., 1979, Geophys. Res. Lett. 6, 566
Webber W.R., Lockwood J.A., Jokipii J.R., 1986, J. Geophys. Res. 91, 4103
Webber W.R., Potgieter M.S., Burger R.A., 1990, ApJ 349, 634
Winterhalter D., Smith E.J., Wolfe J.H., Slavin J.A., 1990, J. Geophys. Res. 95, 1
Zhang G., Burlaga L.F., 1988, J. Geophys. Res. 93, 2511
Zhao X.P., Hundhausen A.J., 1983, J. Geophys. Res. 88, 451